Near-field multilevel physical optics for fast analysis of multi-reflector antennas

Christine Letrou, Amir Boag

Near-Field Multilevel Physical Optics for Fast Analysis of Multi-Reflector Antennas

Christine Letrou[#1], Amir Boag[*2]

[#] *Lab. SAMOVAR (UMR CNRS 5157), TELECOM SudParis*
9 rue Charles Fourier, 91011 Evry cedex, France
[1] `christine.letrou@telecom-sudparis.eu`

[*] *School of Electrical Engineering, Tel Aviv University*
Tel Aviv 69978, Israel
[2] `boag@eng.tau.ac.il`

Abstract—**The MultiLevel Physical Optics (MLPO) algorithm is extended for fast and accurate analysis of multi-reflector antennas. To that end, a near-field version of the MLPO algorithm for field propagation between reflectors is proposed and combined with the earlier developed generalized far-field MLPO. The computational complexity of the near-field MLPO is comparable to that of its far-field counterpart. The performance of the proposed method is studied on the example of RATAN-600 radio telescope antenna.**

I. INTRODUCTION

Very large reflector antennas are often analyzed as quasi-optical systems in two main steps. In the first stage, the field is propagated from the feed to the equivalent aperture, while in the second, the radiation pattern is computed by aperture integration, which for planar apertures can be accelerated using the Fast Fourier Transform (FFT) [1]. The recently developed far-field Multi-Level Physical Optics (MLPO) algorithm [2] facilitates the fast computation of the radiation patterns from given field distributions on non-planar surfaces, thus obviating the need to use planar equivalent apertures that introduce additional phase errors [1]. In order to improve the far sidelobe accuracy, the Physical Theory of Diffraction (PTD) line integral can be included in these computations as described in [3].

In this paper we focus on the first step of the analysis involving the aperture field computation. Conventionally, the field originating from the feed is propagated through successive reflections within a multi-reflector antenna using Geometrical Optics (GO)-based ray tracing [1]. Such GO modeling completely neglects the effects of finite wavelength on the field distributions, thus resulting in significant errors. As an alternative, we propose a numerically efficient near-field MLPO algorithm for accurate field propagation in multi-reflector systems.

II. PROBLEM SPECIFICATION

Consider a multi-reflector antenna comprising N_{ref} perfectly conducting reflecting surfaces $S^{(i)}$, $i = 1,...,N_{\text{ref}}$. The reflectors are enumerated in a sequential order, i.e., the first subreflector $S^{(1)}$ is illuminated by the feed, reflector $S^{(i)}$

illuminates $S^{(i+1)}$, while the main reflector $S^{(N_{\text{ref}})}$ is designed to produce the far-field pattern. Geometry of the RATAN-600 radio telescope antenna, which represents a computationally challenging example of a very large multi-reflector antenna and serves as a test case in our work, is depicted in Fig. 1. We assume that the reflector surfaces are sufficiently smooth as will be detailed below. Harmonic time dependence $e^{j\omega t}$ is assumed and suppressed (with the corresponding frequency $\omega = 2\pi f$ and wavenumber $k = \omega / c$ with c designating the speed of light). Our goal is to compute the radiation pattern of the whole antenna $U(\hat{r})$ for a range of observation directions $\hat{r} = (\sin\theta\cos\varphi, \sin\theta\sin\varphi, \cos\theta)$ at a given frequency. The radiation pattern is conventionally defined via the far field $E(r)$ as $U(\hat{r}) = 4\pi r e^{jkr} E(r)$ for $r \to \infty$ where (r, θ, φ) designate the spherical coordinates of the observation point r. We consider the task of computing the radiation pattern over a given angular sector $\varphi \in [\varphi_{\min}, \varphi_{\max}]$ and $\theta \in [\theta_{\min}, \theta_{\max}]$. The total radiation pattern can be obtained as a superposition of the direct feed radiation and the partial patterns due to the currents induced on each of the reflecting surfaces. Thus, we have

$$U(\hat{r}) = U^{\text{f}}(\hat{r})e^{jk\hat{r}\cdot r^{(\text{f})}} + \sum_{i=1}^{N_{\text{ref}}} U^{(i)}(\hat{r})e^{jk\hat{r}\cdot r^{(i)}} \qquad (1)$$

where $U^{\text{f}}(\hat{r})$ is the radiation pattern of the feed and $U^{(i)}(\hat{r})$ denotes the radiation pattern due to the currents residing on $S^{(i)}$. Note that in (1), we assume that the radiation patterns of the feed and of the *i*th reflector are originally expressed in the local coordinate systems that are centered at $r^{(\text{f})}$ and $r^{(i)}$, which denote the centers of the smallest spheres circumscribing the feed and reflector $S^{(i)}$, respectively. In the PO approximation for PEC surfaces, the far-field radiation pattern of the *i*th reflector centered at $r^{(i)}$ can be computed as

$$U^{(i)}(\hat{r}) = \int_{S^{(i)}} A^{(i)}(\hat{r}, r')e^{jk\hat{r}\cdot(r'-r^{(i)})}ds' \qquad (2)$$

with $A^{(i)}(\hat{r}, r') = j2k\eta\hat{r}\times[\hat{r}\times(\hat{n}'\times H_{\text{inc}}^{(i)})]$ where $H_{\text{inc}}^{(i)}$ and $\hat{n}'$ denote the incident magnetic field and the unit normal vector at the integration point r', respectively.

The incident fields needed for the evaluation of the radiation pattern via (2), can be computed in a sequential

manner starting with the feed radiation. In this work, we assume that $\boldsymbol{U}^{\mathrm{f}}$ and, consequently, $\boldsymbol{H}_{\mathrm{inc}}^{(1)}$ are known. Thus, one can turn to a sequential field propagation from $S^{(i)}$ to $S^{(i+1)}$ for $i = 1, \ldots, N_{\mathrm{ref}} - 1$. Indeed, for a well-designed antenna, the magnetic field $\boldsymbol{H}^{(i)}$ radiated by $S^{(i)}$ dominates the field incident upon $S^{(i+1)}$, i.e., $\boldsymbol{H}_{\mathrm{inc}}^{(i+1)} = \boldsymbol{H}^{(i)}$. In the near-field PO approximation, the magnetic field at point $\boldsymbol{r}$ on surface $S^{(i+1)}$ due to the currents on $S^{(i)}$ is given by

$$\boldsymbol{H}^{(i)}(\boldsymbol{r}) = \int_{S^{(i)}} \boldsymbol{h}(\boldsymbol{r}, \boldsymbol{r}') \frac{e^{-jk|\boldsymbol{r} - \boldsymbol{r}'|}}{|\boldsymbol{r} - \boldsymbol{r}'|} ds' \qquad (3)$$

where

$$\boldsymbol{h}(\boldsymbol{r}, \boldsymbol{r}') = -\frac{jk}{2\pi} \hat{\boldsymbol{r}}' \times (\hat{\boldsymbol{n}}' \times \boldsymbol{H}_{\mathrm{inc}}^{(i)}) \left(1 + \frac{1}{jk|\boldsymbol{r} - \boldsymbol{r}'|} \right) \quad (4)$$

and $\hat{\boldsymbol{r}}' = (\boldsymbol{r} - \boldsymbol{r}')/|\boldsymbol{r} - \boldsymbol{r}'|$. This computational process can be performed sequentially until the field on the main reflector, $\boldsymbol{H}_{\mathrm{inc}}^{(N_{\mathrm{ref}})} = \boldsymbol{H}^{(N_{\mathrm{ref}} - 1)}$, is obtained. The radiation pattern can then be evaluated via (2) and (1). The total complexity of the direct computation is dominated by two asymptotically identical terms of $O(N_{\mathrm{ref}} N^4)$ stemming from the field propagation using (3) and radiation pattern evaluation via (2) each repeated for all reflectors. As a large parameter for the asymptotic complexity estimates, we use $N = kR$ where R is the radius of the minimum sphere circumscribing the antenna.

The far-field MLPO algorithm facilitating fast individual reflector radiation pattern evaluation and subsequent aggregation has been recently presented in [3]. This algorithm reduces the computational costs incurred in the radiation pattern evaluation via (2) and (1) for all reflectors from $O(N_{\mathrm{ref}} N^4)$ to $O(N_{\mathrm{ref}} N^2 \log N)$. Note that the relative sizes of the reflectors are included in the constant factor hidden in these asymptotic estimates. In the next section, we extend the MLPO algorithm to facilitate fast near-field computations that are needed for the field propagation between the reflectors using (3), and otherwise become a bottleneck of the whole computational process.

III. NEAR-FIELD MLPO ALGORITHM

In this section we focus on the computational task of the field propagation from one reflector to the other performed by evaluating the near-field physical optics integral in (3) over $S^{(i)}$ for $O(N^2)$ observation points distributed over the reflector surface $S^{(i+1)}$. As a preprocessing step, we perform a hierarchical domain decomposition of the radiating surface, $S^{(i)}$. Let $\overline{S}_n^L$ with $L = 0, \ldots, M$ and $n = 1, \ldots, N^L$ denote the nth sub-domain of level L, where N^L is the number of sub-domains on level L. The zeroth level comprises only one subdomain, which represents the whole surface, $\overline{S}_1^0 = S^{(i)}$. By each decomposition of a parent subdomain into children

subdomains, we seek to reduce the linear size of the subdomains roughly by a factor of two. Therefore, the resulting structure can be conventionally depicted as a quad-tree. An adaptive subdivision scheme is envisioned for highly elongated reflectors, thus producing slight deviations from the quad-tree structure. The subdivision process continues until the finest level, M, is reached, where subdomains become roughly one wavelength in size.

To obtain the total field, we aggregate the partial fields produced by the sources restricted to the subdomains through a multilevel interpolation process. Let $\overline{\boldsymbol{H}}_n^L(\boldsymbol{r})$ denote the partial magnetic field produced by the PO equivalent currents restricted to subdomain $\overline{S}_n^L$ of $S^{(i)}$. For the smallest subdomains (on level $L = M$), the fields $\overline{\boldsymbol{H}}_n^M(\boldsymbol{r})$, $n = 1, \ldots, N^M$ are evaluated using (3) with $\overline{S}_n^M$ replacing $S^{(i)}$. For all other levels from $L = M - 1$ to 0 in the descending order, we sequentially aggregate fields of children subdomains into those of their parents, until we obtain the total field $\boldsymbol{H}^{(i)} = \overline{\boldsymbol{H}}_1^0$. In order to produce computational savings, we need to consider the rapid spatial variations of the partial fields $\overline{\boldsymbol{H}}_n^L(\boldsymbol{r})$. This behavior is mainly caused by the presence of the Green's function $e^{-jk|\boldsymbol{r} - \boldsymbol{r}'|}/|\boldsymbol{r} - \boldsymbol{r}'|$ in the integrand in (3). The oscillatory behavior can be largely removed by defining a phase and amplitude compensated field

$$\tilde{\boldsymbol{H}}_n^L(\boldsymbol{r}) = \tilde{r}_n^L(\boldsymbol{r}) e^{jk\tilde{r}_n^L(\boldsymbol{r})} \overline{\boldsymbol{H}}_n^L(\boldsymbol{r}) \qquad (5)$$

where $\tilde{r}_n^L(\boldsymbol{r}) = \sqrt{\left|\boldsymbol{r} - \overline{\boldsymbol{r}}_n^L\right|^2 + \left(\overline{R}_n^L\right)^2 / 2}$. Here, $\overline{\boldsymbol{r}}_n^L$ and $\overline{R}_n^L$ denote the center and the radius of the smallest sphere circumscribing $\overline{S}_n^L$. It has been shown in [4] that for a source distribution confined to subdomain $\overline{S}_n^L$, the fields can be sampled on non-uniform spherical grids with the origin at $\overline{\boldsymbol{r}}_n^L$. The local sampling rates versus the radial and angular spherical coordinates (r, θ, φ) in the $\overline{\boldsymbol{r}}_n^L$ centered coordinate system have been derived in [4]. The sampling grids designed according to [4] allow field evaluation at arbitrary rough surfaces while requiring a full 3D interpolation [4]. On the other hand, more efficient algorithms can be designed if the observation surface is sufficiently smooth and the interpolations can be effected directly over the surface. In order to design a 2D interpolation-based algorithm, we assume that the surface of the reflector $S^{(i+1)}$ has a parametric representation $\boldsymbol{r}^{(i+1)}(\boldsymbol{u})$ where $\boldsymbol{u} = (u_1, u_2)$. We assume that the parametric representation $\boldsymbol{r}^{(i+1)}(\boldsymbol{u})$ is continuously differentiable with uniformly bounded derivatives, i.e., satisfy $|\partial_{u_v} \boldsymbol{r}^{(i+1)}(\boldsymbol{u})| \leq r_{u_v}^{(i+1)}$ with $r_{u_v}^{(i+1)}$, $v = 1, 2$ being constants. Then, the required sampling rates versus the parameters u_v, $v = 1, 2$ are

$$f_{u_v}^{\text{s}(i+1)} = r_{u_v}^{(i+1)} \frac{\Omega k \bar{R}_n^L}{\pi d^{i,i+1}}, \quad v=1,2 \qquad (6)$$

where $d^{i,i+1}$ is the minimal distance between $S^{(i)}$ and $S^{(i+1)}$ and $\Omega > 1$ is an oversampling factor. Using these sampling rates we construct a coarse grid of points on the reflector surface, $S^{(i+1)}$, on which the field $\tilde{H}_n^L$ can be computed. However, the field $\tilde{H}_m^{L-1}$ corresponding to the parent subdomain $\bar{S}_m^{L-1}$ needs to be sampled over a denser grid. Thus, in order to perform the aggregation, the compensated field is computed at the desired parent grid points using a local interpolation. Following the interpolation, we restore the amplitude and phase of the field at the target points. The resulting field values of all children subdomains can now be aggregated on the parents grid. This computational sequence is repeated for all subdomains and levels in the descending order until $\bar{H}_1^0 = H^{(i)}$ is obtained on the finest grid defined by the sampling rates (6) for the whole $S^{(i)}$.

The total complexity of the field propagation from $S^{(i)}$ to $S^{(i+1)}$ behaves as $O(N^2 \log N)$, which for all reflectors accumulates to $O(N_{\text{ref}} N^2 \log N)$. Interestingly, one can observe that the complexity of the near-field computations is similar to that of the radiation pattern evaluation and, thus, the use of the near-field MLPO does not modify the asymptotic complexity of the whole computation.

IV. NUMERICAL RESULTS

The algorithm described above has been applied to the core antenna of the southern sector of RATAN 600 radiotelescope. This antenna comprises the feed, secondary and main reflectors as shown in Fig. 1. Both the secondary and the main are parabolic cylindrical reflectors providing collimation in the vertical and horizontal planes, respectively.

The far field of this dual reflector antenna system has been computed for an operating wavelength of 8 cm. The radius of the smallest sphere circumscribing the secondary reflector is roughly 65λ. The main reflector is clearly not in the far field region of this reflector, whose far field distance is more than 2.5 km. The number of decomposition levels in the multilevel procedure was taken equal to 6 on the secondary reflector, and to 12 on the main reflector, so that the smallest subdomains on these surfaces are circumscribed by spheres with their radii comprised between λ and 2λ.

The total computation time on a single Intel X5650@2.67GHz processor was less than 8 minutes (464 s), with 37.9 s devoted to the near-field computation from the secondary to the main reflector, and 426 s - to the computation of the far field radiated by the main reflector, in an angular region $\theta \in [0°, 0.5°]$ with a rotational symmetry around the z axis, $\varphi \in [0°, 360°]$.

Figs. 2 and 3 present respectively the magnitude of the magnetic field on the main reflector surface (as a function of the projection variables x and y) and the far field radiated by

the antenna system around the main lobe (magnitude of the E-field copolarized and cross-polarized components).
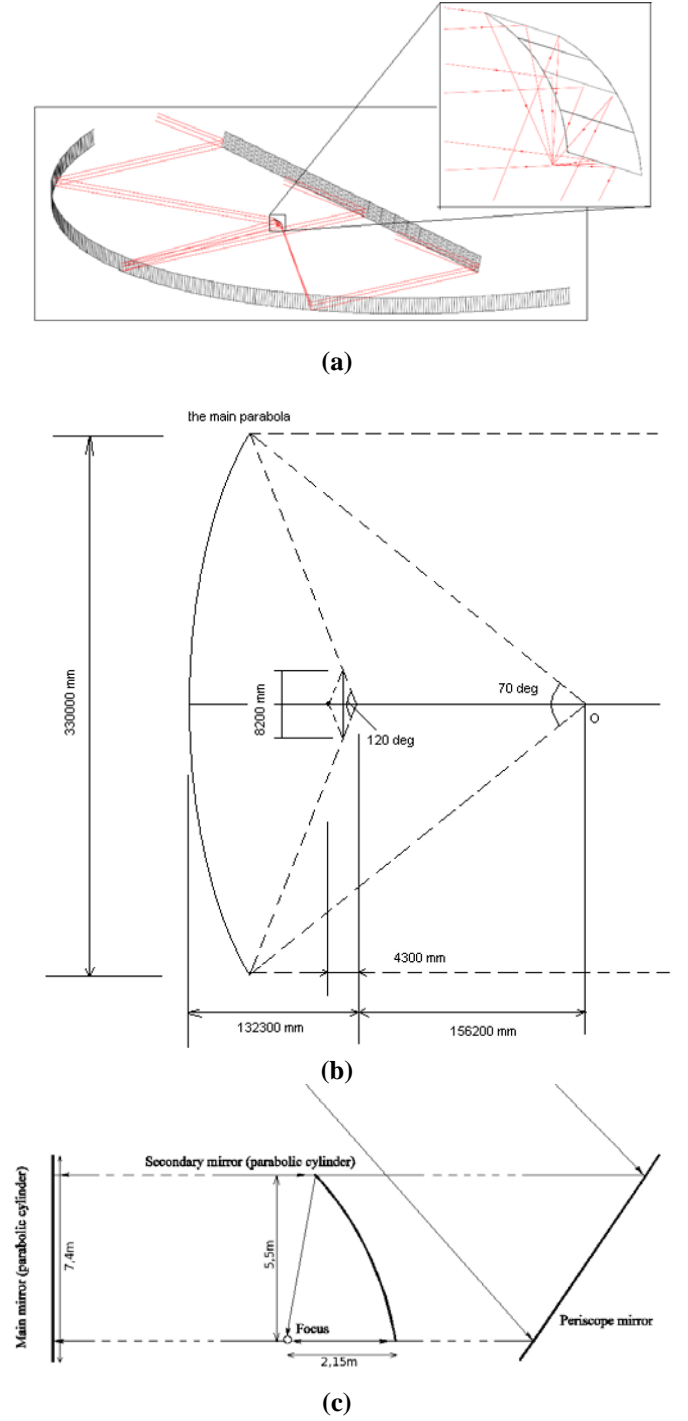
(a)

(b)

(c)

Fig. 1. The primary and secondary reflectors of the RATAN-600 radiotelescope (south sector): (a) Schematic 3D view; (b) Horizontal cut; (c) Vertical cut.
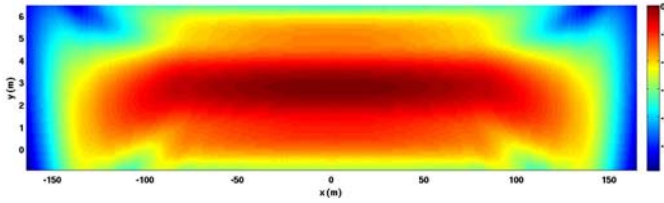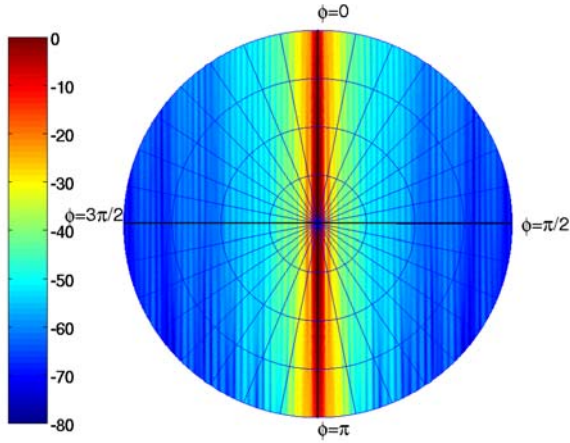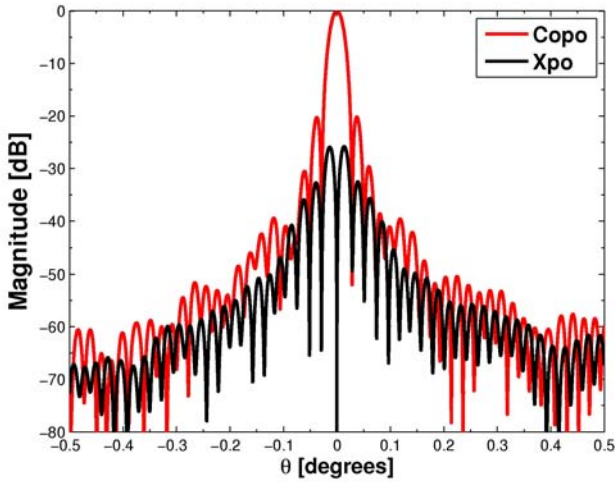
Fig. 2. Magnitude of the magnetic field on the main reflector surface as a function of the projection variables *x* and *y*.

(a)

(b)

Fig. 3. Magnitude of the radiation pattern in the far field of the antenna system: (a) in an angular region $\theta \in [0°, 0.5°]$ and $\varphi \in [0°, 360°]$; (b) Co- and Cross-polarized components along the $\varphi = 90°$ cut.

V. CONCLUSION

A near-field multilevel fast physical optics algorithm has been presented. In this approach, the field propagating from one reflector to the other is computed via a multilevel field aggregation based on phase and amplitude compensated interpolation. Subsequently, the radiation pattern is evaluated using the far-field MLPO developed in an earlier paper [3]. It is shown that the combination of near-field and far-field MLPO algorithms make it possible to perform with controlled accuracy the computation of full 3D patterns of very large multi-reflector antennas.

REFERENCES

[1] R. E. Collin, *Antennas and Radio Wave Propagation*. New York: McGraw-Hill, 1985.
[2] A. Boag and C. Letrou, "Multilevel Fast Physical Optics Algorithm for Radiation from Non-planar Apertures," *IEEE Trans. Antennas Propagat.*, vol. 53, no. 6, pp. 2064-2072, June 2005.
[3] C. Letrou and A. Boag, "Generalized Multilevel Physical Optics (MLPO) for Comprehensive Analysis of Reflector Antennas," *IEEE Trans. Antennas and Propagation*, vol. 60, no. 2, pp. 1182-1186, February 2012.
[4] Y. Brick and A. Boag, "Multilevel non-uniform grid algorithm for acceleration of integral equation based solvers for acoustic scattering," *IEEE Trans. Ultrasonics, Ferroelectrics, and Frequency Control*, vol. 57, no. 1, pp. 262-273, Jan. 2010.